AGU PUBLICATIONS

Geophysical Research Letters

RESEARCH LETTER
10.1002/2014GL061313

Key Points:
- Weddell Sea deep convection ceases with climate change in model simulations
- Cessation of deep convection has strong impact on projected oceanic CO_2 uptake
- Potential of deep convection to cause intermodel spread in oceanic CO_2 uptake

Supporting Information:
- Readme
- Table S1

Correspondence to:
R. Bernardello,
braf@sas.upenn.edu

Citation:
Bernardello, R., I. Marinov, J. B. Palter, E. D. Galbraith, and J. L. Sarmiento (2014), Impact of Weddell Sea deep convection on natural and anthropogenic carbon in a climate model, *Geophys. Res. Lett.*, *41*, 7262–7269, doi:10.1002/2014GL061313.

Received 27 AUG 2014
Accepted 8 OCT 2014
Accepted article online 10 OCT 2014
Published online 27 OCT 2014

Impact of Weddell Sea deep convection on natural and anthropogenic carbon in a climate model

Raffaele Bernardello[1], Irina Marinov[1], Jaime B. Palter[2], Eric D. Galbraith[3], and Jorge L. Sarmiento[4]

[1]Department of Earth and Environmental Science, University of Pennsylvania, Philadelphia, Pennsylvania, USA, [2]Department of Atmospheric and Oceanic Sciences, McGill University, Montreal, Quebec, Canada, [3]Department of Earth and Planetary Sciences, McGill University, Montreal, Quebec, Canada, [4]Atmospheric and Oceanic Sciences Program, Princeton University, Princeton, New Jersey, USA

Abstract A climate model is used to investigate the influence of Weddell Sea open ocean deep convection on anthropogenic and natural carbon uptake for the period 1860–2100. In a three-member ensemble climate change simulation, convection ceases on average by year 1981, weakening the net oceanic cumulative uptake of atmospheric CO_2 by year 2100 (−4.3 Pg C) relative to an ocean that has continued convection. This net weakening results from a decrease in anthropogenic carbon uptake (−10.1 Pg C), partly offset by an increase in natural carbon storage (+5.8 Pg C). Despite representing only 4% of its area, the Weddell Sea is responsible for 22% of the Southern Ocean decrease in total climate-driven carbon uptake and 52% of the decrease in the anthropogenic component of oceanic uptake. Although this is a model-specific result, it illustrates the potential of deep convection to produce an intermodel spread in future projections of ocean carbon uptake.

1. Introduction

The high-latitude Southern Ocean (SO) is thought to play a pivotal role in the preindustrial air-sea partitioning of carbon because of its ability to connect the atmosphere to the vast volume of the deep ocean through the formation of Antarctic Bottom Water (AABW) [*Sarmiento and Toggweiler*, 1984; *Sarmiento and Orr*, 1991; *Marinov et al.*, 2006; *Séférian et al.*, 2012]. However, discrepancies among different techniques to estimate ocean (C_{ant}) content are especially pronounced for deep waters of southern origin, making the role of AABW uncertain [*Vazquez-Rodriguez et al.*, 2009].

AABW presently forms at specific locations on the Antarctic continental shelf [*Orsi et al.*, 1999], while, in the past, this water mass was also known to form during open ocean deep convection events in the Weddell Sea (WS) [*Martinson et al.*, 1981; *Gordon*, 1982; *Killworth*, 1983]. The open ocean convective pathway of AABW was well-documented in satellite observations which revealed an ice-free, convective region in the WS with a size of $2–3 \times 10^5$ km^2 for three consecutive winters in the 1970s [*Carsey*, 1980]. The absence of this pathway in the last 40 years coincides with observed freshening and stratification of the SO [*de Lavergne et al.*, 2014], and warming and volume loss from the AABW layer, possibly linked with a slowdown in its formation rate [*Purkey and Johnson*, 2012].

Meanwhile, open ocean convection in the WS is a prominent feature of many climate models under preindustrial forcing [*Heuze et al.*, 2013]. It is important to note that the coarse resolution hampers the correct representation of shelf processes in global models and therefore may place too much importance on deep open ocean convection. Nonetheless, deep convection has been shown to weaken and cease in warming simulations [*de Lavergne et al.*, 2014], raising the specter of a warming-induced perturbation to ocean carbon uptake and storage. These models vary significantly in the strength and duration of open ocean convection and its sensitivity to warming. Importantly, the timing of the slowdown may give rise to intermodel spread in the evolution of the modeled air-sea exchange of CO_2. Although previous studies have used a water mass framework to characterize the SO carbon uptake [e.g., *Séférian et al.*, 2012], the specific role of subpolar SO deep convection on air-sea CO_2 exchange in models has yet to be explored.

Here we use a coupled climate model to understand the role of WS convection and its disappearance on the ocean's storage of natural and anthropogenic carbon. Because our model simulates WS convection events under preindustrial conditions [*Galbraith et al.*, 2011] and their abrupt cessation under warming

[*Bernardello et al.*, 2014; *de Lavergne et al.*, 2014], it provides an ideal tool for exploring these potential feedbacks to the simulated carbon cycle.

The response of ocean carbon uptake to changes in deep ocean convection is complex. During Weddell Sea convection AABW is formed through heat loss from Circumpolar Deep Water (CDW) exposed to the atmosphere. CDW has, on average, been isolated from the surface of the ocean for millennia [*DeVries and Primeau*, 2011]. During this time, CDW accumulates high dissolved inorganic carbon (DIC) concentrations as a consequence of the remineralization of sinking particulate organic matter. Because of these high DIC concentrations, a WS convection event would be expected to produce a transient rise in atmospheric CO_2 via natural carbon (C_{nat}) outgassing from newly exposed, supersaturated CDW prior to the anthropogenic addition of CO_2 to the atmosphere. This transient rise in atmospheric CO_2 would be counterbalanced partly by the reestablishment of an equilibrium between the atmosphere and surface mixed layer and partly by the accumulation of remineralized carbon in the deep global ocean, leading to a steady state on timescales longer than those of convection. Thus, the suppression of convection-driven outgassing under anthropogenic warming might represent a negative feedback on atmospheric CO_2 by allowing the ocean to retain an increasing load of remineralized DIC. However, there is also a positive feedback that occurs from reduced oceanic uptake of C_{ant} in a nonconvecting ocean, as will be described below. Hence, the expected net cumulative effect of the suppression of open ocean deep convection on global ocean CO_2 uptake is far from obvious.

After describing the model and our simulation design (section 2), we synthesize the impact of convection on C_{nat} storage in the WS under preindustrial conditions (section 3) and the implications of a climate-driven convective shutdown on air-sea CO_2 fluxes (section 4). Finally, we offer conclusions and explore additional questions left for future study in section 5.

2. Model and Simulation Design

All simulations were carried out using CM2MC [*Galbraith et al.*, 2011], the Geophysical Fluid Dynamics Laboratory Climate Model version 2 with Modular Ocean Model version 4p1 at coarse resolution. CM2Mc uses the same physical oceanic and atmospheric code as the Earth System Model with the Modular Ocean Model (ESM2M) [*Dunne et al.*, 2012], with minor alterations as required to adjust to the coarser discretization. The CM2Mc ocean uses a tripolar grid with nominal 3° resolution and 28 vertical levels with a finer resolution toward the surface. Eddy mixing is parameterized following *Gent and McWilliams* [1990] with a spatially varying diffusion coefficient [*Griffies et al.*, 2005]. Ocean biogeochemistry is solved by the Biogeochemistry with Light, Iron, Nutrients, and Gases model, with a representation of carbon chemistry [*Galbraith et al.*, 2010; *Bernardello et al.*, 2014].

The model was initialized as described in *Galbraith et al.* [2011] and spun-up for 4500 years. In order to account for sensitivity to initial conditions, we extracted atmospheric and oceanic conditions at three points during the last 1000 years of the spin-up: immediately before, during, and after a convection period. These three states were used to initialize three independent simulations, producing an ensemble, under each of the following four scenarios:

A. *Warming_increasingCO_2*: A climate change simulation using prescribed atmospheric concentrations for greenhouse gases and aerosols recommended by the Coupled Model Intercomparison Project Phase 5 (CMIP5). We use the historical forcing (1860–2005) and the Representative Concentration Pathway 8.5 (2006–2100), detailed in *Meinshausen et al.* [2011]. Ozone, including contemporary depletion and its predicted future recovery, is also prescribed [*Cionni et al.*, 2011].

B. *Warming_constantCO_2*: In this simulation, the climate responds to the radiative forcing due to historical+RCP8.5, but the ocean chemistry is not affected by the rise in atmospheric CO_2.

C. *Control_increasingCO_2*: A preindustrial climate simulation, where greenhouse gases, aerosols, and ozone are kept at the value of year 1860. However, ocean chemistry is affected by the increase in atmospheric CO_2 according to Historical+RCP8.5, allowing C_{ant} to invade the ocean through air-sea gas exchange.

D. *Control_constantCO_2*: A preindustrial control simulation, in which radiative forcing is at preindustrial level (as in Control_increasingCO_2) and ocean chemistry responds to a constant preindustrial atmospheric CO_2 concentration (as in Warming_constantCO_2).

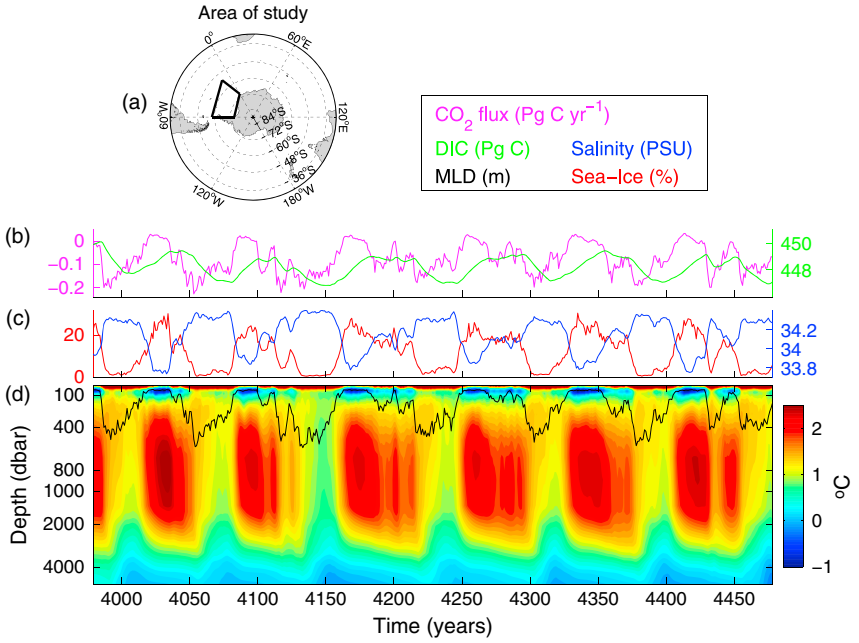

Figure 1. Yearly averaged Weddell Sea convection cycles in a 500 year segment of preindustrial simulation. (a) Area of study; (b) area-integrated CO_2 flux and total mass of DIC inside the study area; averages of the study area for (c) sea ice concentration and salinity (average 0–50 m depth); (d) water temperature and mixed layer depth.

By comparing the air-sea CO_2 fluxes (ϕ), integrated over the area of study (Figure 1a), in these simulations, we can quantify the direct impact of the suppression of WS convection on the ocean's ability to retain C_{nat} and absorb C_{ant}. The difference between Warming_increasingCO_2 and Control_increasingCO_2 (A − C) reveals the influence of WS convection (among other climate-driven changes in the area) on the total carbon ($C_{ant} + C_{nat}$) ocean uptake ($\Delta\phi_{Total}$), while Warming_constantCO_2 minus Control_constantCO_2 (B − D) reveals the impact on the C_{nat} flux only ($\Delta\phi_{Natural}$). Thus, the difference ((A − C) − (B − D)) reveals the impact of climate change on the C_{ant} uptake ($\Delta\phi_{Total} - \Delta\phi_{Natural} = \Delta\phi_{Anthropogenic}$). For the last 1000 years of the spin-up we saved yearly averaged outputs to investigate the characteristics of regular convective cycles. Monthly averages were saved for simulations A, B, C, and D. Since open ocean convection occurs in winter, we defined a convective year as any year in which the September mixed layer was deeper than 2000 m over any portion of the study area in simulations A, B, C, and D. By comparing the September mixed layer with its annual average, we found that annually averaged mixed layer for nonconvective years was never deeper than 60 m. Therefore, during the 1000 year segment, we used a mixed layer depth threshold of 60 m to distinguish convective from nonconvective years.

CM2Mc response to historical+RCP8.5 forcing is discussed in *Bernardello et al.* [2014] while *de Lavergne et al.* [2014] compare CM2Mc to CMIP5 models and to observations for aspects related to SO deep convection. For the present study we have also calculated mean CM2Mc water masses characteristics following the procedure described by *Sallée et al.* [2013] as a further model evaluation (see supporting information).

3. Effects of the Simulated Weddell Polynya on Climate and Natural Carbon Storage

Under preindustrial conditions, deep convection in the Weddell Sea is characterized by a regular periodicity in CM2Mc, as illustrated by the vertical homogenization of temperature from the surface to 4000 m (Figure 1d). Non-convective periods occur, on average, every 60 years and last for approximately 20 years. During these non-convective periods, warm and salty water originating from CDW is transported into the WS at depth and accumulates between 200 m and 3000 m, creating a temperature inversion that is stabilized by the halocline. Reduced vertical mixing between the surface and this warmer and saltier layer contributes to cooling and freshening at the surface and coincides with an expansion of sea ice (Figure 1c). Because the surface freshening dominates in setting the evolution of the pycnocline during non-convective

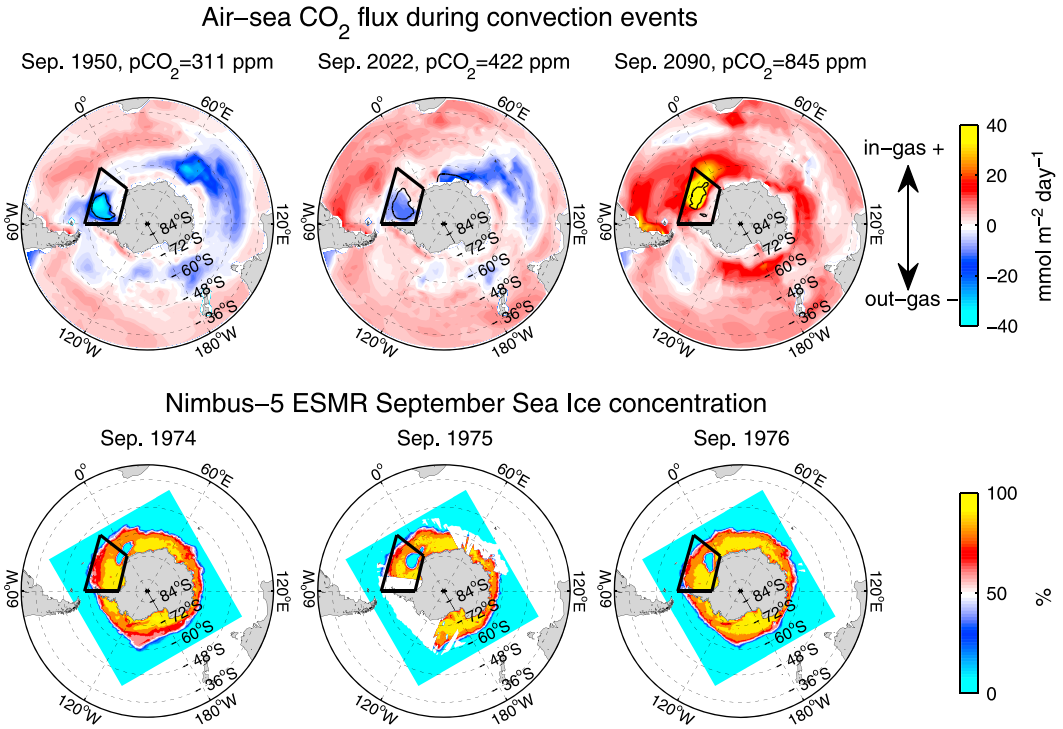

Figure 2. (top row) Modeled air-sea CO_2 flux during September for the Control_increasingCO_2 simulation. Black contours indicate the convecting area (mixed layer depth >2000 m). Three convective years are shown to illustrate how the increase of atmospheric CO_2 gradually weakens the outgassing of CO_2 and eventually turns convective areas to a sink for atmospheric CO_2. (bottom row) Observed Nimbus-5 Electrically Scanning Microwave Radiometer September sea ice concentrations for the three years characterized by the Weddell Sea polynya.

periods, density stratification increases in spite of the subsurface warming. In our model, WS convection is periodically triggered by changes in the precipitation-evaporation balance, which lead to a low-frequency modulation of surface salinity [*Galbraith et al.*, 2011]. Once convection begins, the upward flux of heat from the subsurface ocean prevents the formation of winter sea ice, and a large polynya develops, qualitatively similar to the polynya observed in the 1970s, though often significantly larger (up to 8 times, Figure 2). Its position migrates within the trapezoidal area depicted in Figure 1a, which defines our area of study.

During convective periods, CM2Mc global surface air temperatures rise by 0.4°C relative to nonconvective periods, linked to the heat released from the deep ocean (not shown). A similar response was described for another model that simulates WS convection events with centennial scale variability [*Latif et al.*, 2013]. Furthermore, by exchanging with the vast C_{nat} pool of the deep ocean, each WS convective period promotes an average CO_2 outgassing of about 6.1 Pg C. Over the 60 years of a convective period, this amount of CO_2 corresponds to about 0.1 Pg C yr^{-1} (Figure 1b) and contributes a considerable fraction of the total variability in the preindustrial control simulation: the standard deviation of the globally integrated annual flux of CO_2 in Control_constantCO_2 is just 0.16 Pg C yr^{-1}. Following the heat release, the erosion of the temperature inversion promotes the stabilization of the water column and the reestablishment of a surface halocline. This allows the transition to a nonconvective period, the expansion of sea ice, the steady subsurface accumulation of heat and carbon, and the beginning of a new cycle.

4. Collapse of the Weddell Polynya and Response of the Air-Sea CO_2 Fluxes

In our simulations, surface freshening, resulting from an increased precipitation minus evaporation balance over most of the SO, suppresses deep convection in the WS under historical+RCP8.5 forcing (Figure 3). The last convective year for each of the three ensemble members is 1952, 1987, and 2005. Following this cessation, heat continuously accumulates at depth, but the surface freshening provides increasing stability and prevents the onset of convection until the end of the simulations in 2100. Under preindustrial

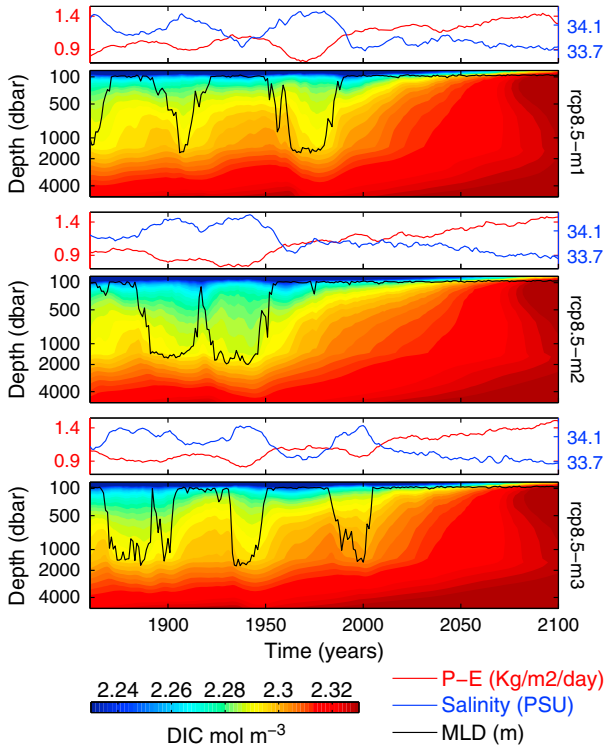

Figure 3. DIC concentration averaged over the study area for the three ensemble members of the Warming_increasingCO_2 simulation. September mixed layer is superimposed (black line). Precipitation-evaporation flux and salinity (average 0–50 m depth) for the same area are also shown for each ensemble member.

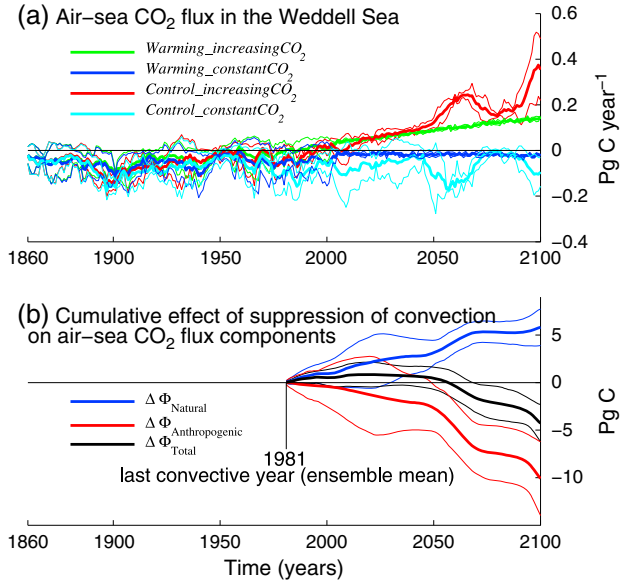

Figure 4. (a) Air-sea CO_2 flux integrated over the area of study for the four simulations. (b) Cumulative climate-driven changes in CO_2 fluxes, calculated from the ensemble averages as: $\Delta\phi_{Natural}$ = Warming_constantCO_2 − Control_constantCO_2 (B − D), $\Delta\phi_{Total}$ = Warming_increasingCO_2 − Control_increasingCO_2 (A − C), $\Delta\phi_{Anthropogenic}=\Delta\phi_{Total} - \Delta\phi_{Natural}$. In both panels thick lines refer to the ensemble mean while thin lines show ± 1 standard deviation relative to the three-member ensemble.

atmospheric CO_2 concentrations, simulated WS deep convective events cause outgassing of C_{nat} (Figure 4a, Control_constantCO_2) because the pCO_2 at the sea surface during these events is higher than its atmospheric counterpart, as expected.

However, in addition to its impact on C_{nat}, the suppression of convection in the WS impacts the uptake and storage of anthropogenic CO_2 from the atmosphere. If open ocean convection persists in spite of rising atmospheric CO_2, as is simulated in Control_increasingCO_2, the CO_2 outgassing during convective events gradually weakens. This weakening begins as soon as anthropogenic emissions start to rise, due to the reduction in the air-sea CO_2 gradient during convective events. When atmospheric pCO_2 climbs to the pCO_2 of the exposed deep waters, the sign of the total flux reaches zero, after which convective events become net ingassing events (Figure 2). Essentially, the pCO_2 of water exposed during deep convection is set by the deep ocean carbon reservoir, which increases very slowly compared to atmospheric pCO_2. Because the atmospheric pCO_2 rises while the pCO_2 of exposed deep waters stays relatively constant, this part of the ocean becomes a sink of anthropogenic CO_2, relative to the preindustrial baseline. The very same deep mixing that released carbon under preindustrial pCO_2 then becomes a conduit that transfers absorbed carbon to depth. This redistribution allows for the continued uptake of anthropogenic CO_2 throughout the duration of the convection event. Thus, anthropogenic CO_2 uptake in the WS is 46% lower when convection is suppressed (last two rows of Table 1).

Additional outgassing regions are visible in the September 1950 snapshot (Figure 2), mainly between 60°E and 120°E in the Indian Ocean sector of the SO. The southernmost area, between 60°S and 48°S, lies within the region of Ekman-driven upwelling where CO_2-rich CDW is transported into the surface mixed layer. Between 48°S and 36°S, the mixed layer deepens along the path of

Table 1. Cumulative Ocean CO_2 Uptake (Ensemble Average 1981–2100) for the Weddell Sea (WS), the Southern Ocean (SO), and the Global Ocean (GO); Effect of Climate Change on Cumulative Ocean CO_2 Uptake Components; and Anthropogenic CO_2 Uptake Without and With Climate Change (Units are Pg C)

	WS	SO	GO
	Cumulative Ocean CO_2 Uptake Between 1981 and 2100		
Warming_increasingCO_2 (A)	+8.9±0.6	+181.9±2.2	+495.4±2.2
Warming_constantCO_2 (B)	−2.8±1	−18.1±2.5	−30.4±2.9
Control_increasingCO_2 (C)	+13.2±1.4	+201.2±2.4	+574.6±2.1
Control_constantCO_2 (D)	−8.6±0.9	−18.1±1.9	−6.3±2.3
	Effect of Climate Change on Cumulative Ocean CO_2 Uptake		
$\Delta\phi_{Natural}$ (B − D)	+5.8±1.9	−0.0±4.3	−24.1±5.2
$\Delta\phi_{Anthropogenic}$ (A − C) − (B − D)	−10.1±3.9	−19.3±8.8	−55.1±9.6
$\Delta\phi_{Total}$ (A − C)	−4.3±1.9	−19.3±4.5	−79.2±4.3
	Anthropogenic CO_2 Uptake Without and With Climate Change		
$\Delta\phi_{Control}$ (C − D)	+21.8±2.3	+219.3±4.2	+580.9±4.4
$\Delta\phi_{Warming}$ (A − B)	+11.7±1.5	+200.0±4.6	+525.8±5.1

the Antarctic Circumpolar Current. Here the CO_2 absorbed upstream is inducted into the deepening mixed layer as described by *Sallée et al.* [2012]. Both mechanisms lead to the strong outgassing seen in the winter of 1950. In the presence of increasing anthropogenic CO_2, the outgassing associated with these mechanisms is reduced and eliminated (Figure 2).

To summarize, in the full climate change simulation (Warming_increasingCO_2), the suppression of WS convection causes reduced cumulated anthropogenic CO_2 uptake (−10.1±3.9 Pg C, Table 1) but simultaneously promotes the added storage of natural CO_2 (+5.8±1.9 Pg C). The net balance is a decrease of cumulative CO_2 uptake of 4.3±1.9 Pg C between 1981 (the last convective year in the ensemble mean) and 2100. The cumulative time evolution of the $\Delta\phi$ components in Figure 4b shows how $\Delta\phi_{Total}$ becomes negative when the decrease in $\Delta\phi_{Anthropogenic}$ due to the absence of convection exceeds the increased storage effect on $\Delta\phi_{Natural}$ by year 2055.

5. Discussion and Conclusions

To put in context the carbon uptake reduction ($\Delta\phi_{Total}$) induced by the cessation of WS convection, one must consider that, despite representing only 4% and 1% of the Southern and global ocean areas, respectively, this region contributes 22% and 5% to their respective climate-induced reduction of CO_2 uptake in our simulations (Table 1). When considering the anthropogenic component alone ($\Delta\phi_{Anthropogenic}$), this contribution goes up to 52% and 18%, respectively.

This large contribution to the modeled reduction in ocean carbon uptake highlights the diversity of processes that lead to a changing ocean carbon sink in our model. As a point of comparison, *Le Quere et al.* [2007] used atmospheric CO_2 observations and an inverse method to diagnose a weakening of the SO CO_2 uptake of 0.08 Pg C yr^{-1} per decade for the period 1981–2004. They attributed this trend to strengthened westerly winds, enhanced upwelling of carbon-rich CDW, and attendant CO_2 outgassing. The influence of the WS convection of the 1970s preceded their analysis. Our ensemble shows a similar weakening of the SO CO_2 uptake of 0.05 Pg C yr^{-1} per decade over the same period. However, over half of the SO carbon sink weakening in our simulations is due to outgassing of C_{nat} during convective events. Thus, while the decline in our ensemble mean ocean carbon uptake is similar to that calculated by *Le Quere et al.* [2007], at least one mechanism for this simulated decline is distinct.

We argue here that SO deep convection in our model (and also in nature in the recent past) represents an alternative route by which C_{nat} exits and C_{ant} enters the ocean, which could be likened to a trap door, directly accessing the deep ocean from the surface. In contrast to the door provided by the wind-driven upwelling [*Russell et al.*, 2006], this trap door is held shut by surface freshening under global warming in many models and has remained shut since the 1970s in nature [*de Lavergne et al.*, 2014].

Considering the wide spectrum of intensity and frequency of SO deep convection in CMIP5 models and the range of their response to climate change [*Heuze et al.*, 2013; *de Lavergne et al.*, 2014], a similarly wide

spectrum in total carbon uptake and C_{ant} interior distribution is to be expected. Roughly a third of models have no SO deep convection during their preindustrial simulations; of the two thirds that do convect, the strength of preindustrial convection and the sensitivity to anthropogenic climate change vary widely [*de Lavergne et al.*, 2014]. The longer simulated deep convection persists in the face of warming, the more C_{ant} is taken up in the SO. Similarly, models with larger areas of convection expose more of their interior ocean volume to high atmospheric pCO_2 and store a higher fraction of the absorbed C_{ant} in AABW. We suggest that variability in SO deep convection could be a major source of intermodel spread for the carbon cycle. Although our results are based on one coarse-resolution model only, our model is near the multimodel average of CMIP5 simulations with respect to the percentage of convective years (66% for CM2Mc and 63% for CMIP5 average) and the size of the convective region during the preindustrial (7.6×10^5 km^2 for CM2Mc and 9.3×10^5 km^2 for CMIP5 average) [*de Lavergne et al.*, 2014], suggesting the impact on the carbon cycle may be fairly representative of the convecting models. However, convection collapses early in the period of historical forcing relative to many of the models, which we would expect to lead to large weakening of the oceanic C_{ant} sink.

In summary, we have shown that deep convection in the polar SO has a strong impact on the global ocean carbon uptake in transient climate simulations with a climate model. Considering that deep convection in the polar SO is a common and widely variable feature among the latest generation of climate models we stress here the necessity to better understand its role in determining the intermodel spread in ocean carbon uptake. The development of proxy records for past variability in Southern Ocean deep convection would allow better characterization of this process in the real world.

Acknowledgments

Output from CM2Mc simulations used for this study are available upon request from the corresponding author, R.B. (raffer@noc.ac.uk). R.B. and I.M. were sponsored by NOAA grant NOAA-NA10OAR4310092. J.B.P. was supported by the Natural Sciences and Engineering Research Council (NSERC). E.G. was supported by the Canadian Institute for Advanced Research (CIFAR) and NSERC. This work was partially supported by the Carbon Mitigation Initiative (CMI) project at Princeton University, sponsored by B.P.

Peter Strutton thanks Wolfgang Koeve and one anonymous reviewer for their assistance in evaluating this paper.

References

Bernardello, R., I. Marinov, J. Palter, J. Sarmiento, E. Galbraith, and R. Slater (2014), Response of the ocean natural carbon storage to projected twenty-first-century climate change, *J. Clim.*, *27*, 2033–2053, doi:10.1175/JCLI-D-13-00343.1.

Carsey, F. (1980), Microwave observation of the Weddell Polynya, *Mon. Weather Rev.*, *108*(12), 2032–2044, doi:10.1175/1520-0493(1980)108<2032:MOOTWP>2.0.CO;2.

Cionni, I., V. Eyring, J. F. Lamarque, W. J. Randel, D. S. Stevenson, F. Wu, G. E. Bodeker, T. G. Shepherd, D. T. Shindell, and D. W. Waugh (2011), Ozone database in support of CMIP5 simulations: Results and corresponding radiative forcing, *Atmos. Chem. Phys.*, *11*(21), 11,267–11,292, doi:10.5194/acp-11-11267-2011.

de Lavergne, C., J. Palter, E. Galbraith, R. Bernardello, and I. Marinov (2014), Cessation of deep convection in the open Southern Ocean under anthropogenic climate change, *Nat. Clim. Change*, *4*, 278–282, doi:10.1038/nclimate2132.

DeVries, T., and F. Primeau (2011), Dynamically and observationally constrained estimates of water-mass distributions and ages in the global ocean, *J. Phys. Oceanogr.*, *41*(12), 2381–2401, doi:10.1175/JPO-D-10-05011.1.

Dunne, J. P., et al. (2012), GFDL's ESM2 global coupled climate-carbon Earth system models. Part I: Physical formulation and baseline simulation characteristics, *J. Clim.*, *25*(19), 6646–6665, doi:10.1175/JCLI-D-11-00560.1.

Galbraith, E. D., A. Gnanadesikan, J. P. Dunne, and M. R. Hiscock (2010), Regional impacts of iron-light colimitation in a global biogeochemical model, *Biogeosciences*, *7*(3), 1043–1064.

Galbraith, E. D., et al. (2011), Climate variability and radiocarbon in the CM2Mc Earth system model, *J. Clim.*, *24*(16), 4230–4254, doi:10.1175/2011JCLI3919.1.

Gent, P. R., and J. C. McWilliams (1990), Isopycnal mixing in ocean circulation models, *J. Phys. Oceanogr.*, *20*(1), 150–155, doi:10.1175/1520-0485(1990)020<0150:IMIOCM>2.0.CO;2.

Gordon, A. L. (1982), Weddell deep water variability, *J. Mar. Res.*, *40*(S), 199–217.

Griffies, S. M., et al. (2005), Formulation of an ocean model for global climate simulations, *Ocean Sci.*, *1*(1), 45–79.

Heuze, C., K. J. Heywood, D. P. Stevens, and J. K. Ridley (2013), Southern Ocean bottom water characteristics in CMIP5 models, *Geophys. Res. Lett.*, *40*, 1409–1414, doi:10.1002/grl.50287.

Killworth, P. (1983), Deep convection in the world ocean, *Rev. Geophys.*, *21*(1), 1–26, doi:10.1029/RG021i001p00001.

Latif, M., T. Martin, and W. Park (2013), Southern Ocean sector centennial climate variability and recent decadal trends, *J. Clim.*, *26*(19), 7767–7782, doi:10.1175/JCLI-D-12-00281.1.

Le Quere, C., et al. (2007), Saturation of the Southern Ocean CO_2 sink due to recent climate change, *Science*, *316*(5832), 1735–1738, doi:10.1126/science.1136188.

Marinov, I., A. Gnanadesikan, J. Toggweiler, and J. Sarmiento (2006), The Southern Ocean biogeochemical divide, *Nature*, *441*(7096), 964–967, doi:10.1038/nature04883.

Martinson, D., P. Killworth, and A. Gordon (1981), A convective model for the Weddell Polynya, *J. Phys. Oceanogr.*, *11*(4), 466–488, doi:10.1175/1520-0485(1981)011<0466:ACMFTW>2.0.CO;2.

Meinshausen, M., et al. (2011), The RCP greenhouse gas concentrations and their extensions from 1765 to 2300, *Clim. Change*, *109*(1-2), 213–241, doi:10.1007/s10584-011-0156-z.

Orsi, A., G. Johnson, and J. Bullister (1999), Circulation, mixing, and production of Antarctic bottom water, *Prog. Oceanogr.*, *43*(1), 55–109, doi:10.1016/S0079-6611(99)00004-X.

Purkey, S. G., and G. C. Johnson (2012), Global contraction of Antarctic bottom water between the 1980s and 2000s, *J. Clim.*, *25*(17), 5830–5844, doi:10.1175/JCLI-D-11-00612.1.

Russell, J. L., R. J. Stouffer, and K. W. Dixon (2006), Intercomparison of the Southern Ocean circulations in IPCC coupled model control simulations, *J. Clim.*, *19*(18), 4560–4575.

Sallée, J.-B., R. J. Matear, S. R. Rintoul, and A. Lenton (2012), Localized subduction of anthropogenic carbon dioxide in the Southern Hemisphere oceans, *Nat. Geosci.*, *5*(8), 579–584, doi:10.1038/NGEO1523.

Sallée, J.-B., E. Shuckburgh, N. Bruneau, A. J. S. Meijers, T. J. Bracegirdle, Z. Wang, and T. Roy (2013), Assessment of Southern Ocean water mass circulation and characteristics in CMIP5 models: Historical bias and forcing response, *J. Geophys. Res. Oceans*, *118*(4), 1830–1844, doi:10.1002/jgrc.20135.

Sarmiento, J., and J. Orr (1991), Three-dimensional simulations of the impact of Southern Ocean nutrient depletion on atmospheric CO_2 and ocean chemistry, *Limnol. Oceanogr.*, *36*(8), 1928–1950.

Sarmiento, J., and J. Toggweiler (1984), A new model for the role of the oceans in determining atmospheric pCO_2, *Nature*, *308*(5960), 621–624, doi:10.1038/308621a0.

Séférian, R., D. Iudicone, L. Bopp, T. Roy, and G. Madec (2012), Water mass analysis of effect of climate change on air-sea CO_2 fluxes: The Southern Ocean, *J. Clim.*, *25*, 3894–3908, doi:10.1175/JCLI-D-11-00291.1.

Vazquez-Rodriguez, M., F. Touratier, C. Lo Monaco, D. W. Waugh, X. A. Padin, R. G. J. Bellerby, C. Goyet, N. Metzl, A. F. Rios, and F. F. Perez (2009), Anthropogenic carbon distributions in the Atlantic Ocean: Data-based estimates from the Arctic to the Antarctic, *Biogeosciences*, *6*(3), 439–451.